Pleckstrin Homology Domain Diffusion in Dictyostelium Cytoplasm Studied Using Fluorescence Correlation Spectroscopy

Engel, Ruchira; Hink, Mark A.; Bosgraaf, Leonard; Haastert, Peter J.M. van; Visser, Antonie J.W.G.

Published in:
The Journal of Biological Chemistry

DOI:
10.1074/jbc.M310039200

THE JOURNAL OF BIOLOGICAL CHEMISTRY
Vol. 279, No. 11, Issue of March 12, pp. 10013–10019, 2004

Printed in U.S.A.

Pleckstrin Homology Domain Diffusion in *Dictyostelium* Cytoplasm Studied Using Fluorescence Correlation Spectroscopy*

Received for publication, September 10, 2003, and in revised form, December 18, 2003
Published, JBC Papers in Press, December 29, 2003, DOI 10.1074/jbc.M310039200

Ruchira‡§, Mark A. Hink‡, Leonard Bosgraaf¶, Peter J. M. van Haastert¶, and Antonie J. W. G. Visser‡

From the ‡MicroSpectroscopy Centre, Laboratory of Biochemistry, Wageningen University, Dreijenlaan 3, 6703 HA Wageningen, The Netherlands and the ¶Department of Biochemistry, University of Groningen, Nijenborgh 4, 9747 AG Groningen, The Netherlands

The translocation of pleckstrin homology (PH) domain-containing proteins from the cytoplasm to the plasma membrane plays an important role in the chemotaxis mechanism of *Dictyostelium* cells. The diffusion of three PH domain-green fluorescent protein (GFP) fusions (PH2-GFP, PH10-GFP, and PH-CRAC (cytosolic regulator of adenylyl cyclase)-GFP) in the cytoplasm of vegetative and chemotaxing *Dictyostelium* cells has been studied using fluorescence correlation spectroscopy to gain a better understanding of the functioning of the domains and to assess the effect of initiation of chemotaxis on these domains in the cell. PH2-GFP was homogeneously distributed in vegetative as well as chemotaxing cells, whereas PH10-GFP and PH-CRAC-GFP showed translocation to the leading edge of the chemotaxing cell. The diffusion characteristics of PH2-GFP and PH-CRAC-GFP were very similar; however, PH10-GFP exhibited slower diffusion. Photon counting histogram statistics show that this slow diffusion was not due to aggregation. Diffusion of the three PH domains was affected to similar extents by intracellular heterogeneities in vegetative as well as chemotaxing cells. From the diffusion of free cytoplasmic GFP, it was calculated that the viscosity in chemotaxing cells was 1.7 times lower than in vegetative cells. In chemotaxing cells, PH2-GFP showed increased mobility, whereas the mobilities of PH10-GFP and PH-CRAC-GFP remained unchanged.

The social ameba *Dictyostelium discoideum* begins its life as single cells, feeding on bacteria. When the food supply is exhausted, starvation induces the single cells to aggregate and to develop, eventually forming a multicellular organism. Aggregation of cells is governed by chemotaxis to cAMP. During chemotaxis, cellular movement is mediated by pseudopod formation that results from the activation of several second messenger pathways in response to the binding of cAMP to the receptor. It is thought that one crucial step leading to pseudopod formation is the activation of phosphatidylinositol 3-kinase, which generates negatively charged phospholipids that act as binding sites for pleckstrin homology (PH)[1] domains at the plasma membrane (1). PH domains are homologous regions of ~120 amino acids found in a number of proteins that are quite diverse in their cellular functions. Although the level of sequence similarity between different PH domains is quite low, the secondary structures of the domains are very similar. PH domains can form electrostatically polarized tertiary structure that can interact with negatively charged membrane surfaces. Apart from phospholipids, the $\beta\gamma$-subunits of heterotrimeric G-proteins and protein kinase C have been proposed as common ligands for PH domains. PH domains are thought to be responsible for translocation of cytosolic PH domain-containing proteins to the plasma membrane, where they can initiate further action (2–4). Chemotaxing *Dictyostelium* cells are polarized. It has been suggested that the directional response of the *Dictyostelium* cell comes from the selective recruitment of certain PH domain-containing proteins to the leading edge (1, 5). Although PH domains are known to play a very important role in the process of chemotaxis, very little is known about the dynamics of these domains in cells. Thus, we do not know if PH domains that have different functions in the cell would still show similar diffusion behavior, a property that depends on the structure, localization, and intracellular interactions of the domain in the cell. Also, upon initiation of chemotaxis, it is not known how these diffusion characteristics would be affected. In polarized *Dictyostelium* cells, the formation of pseudopods may lead to change in fluidity of cytoplasm or generation of force due to reorganization of the cytoskeleton. The changes in the intracellular environment upon polarization of the cell would affect the various intracellular species. A study by Potma *et al.* (6) has demonstrated that, due to reduction of actin cytoskeleton in the non-cortical regions of polarized *Dictyostelium* cells, free green fluorescent protein (GFP) in these regions shows faster mobility than in vegetative cells. The altered environment in the cell should also affect the PH domains. Quantifying the diffusion characteristics of the species of interest in vegetative cells and determining the changes in these characteristics upon polarization of the cells would thus provide information not only about the dynamics of different PH domains and their possible interactions with other intracellular moieties, but also about the effect of cell polarization.

The technique of choice for obtaining quantitative information on dynamic events in living cells in a noninvasive manner is fluorescence correlation spectroscopy (FCS) (7). FCS has been applied successfully to quantify the diffusion rates of cellular moieties (8–12). Along with FCS, the complementary technique photon counting histogram (PCH) analysis can be used to provide additional information about the system, *e.g.* the aggregation state of the fluorescent species in the system

* This work was financially supported by the Research Council for Earth and Life Sciences of Netherlands Organization for Scientific Research. The costs of publication of this article were defrayed in part by the payment of page charges. This article must therefore be hereby marked "*advertisement*" in accordance with 18 U.S.C. Section 1734 solely to indicate this fact.

§ To whom correspondence should be addressed. Tel.: 31-317-484701; Fax: 31-317-484801; E-mail: ru.ruchira@wur.nl.

[1] The abbreviations used are: PH, pleckstrin homology; GFP, green fluorescent protein; FCS, fluorescence correlation spectroscopy; PCH, photon counting histogram.

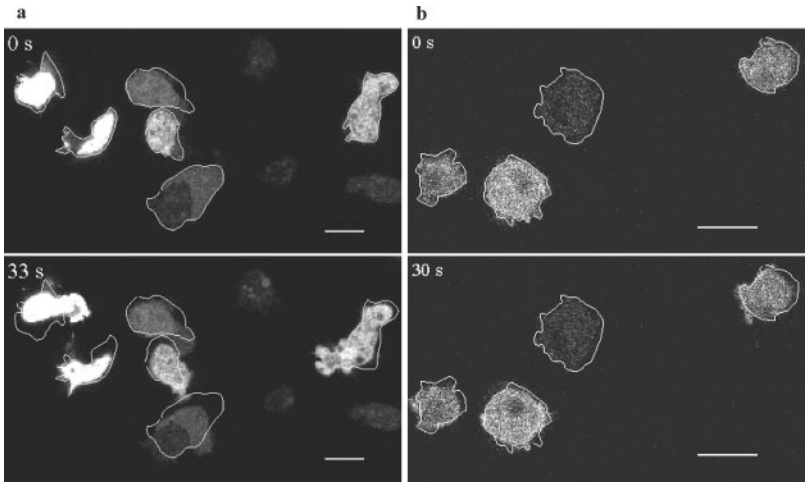

FIG. 1. **Cell immobilization.** Shown are confocal images of vegetative *Dictyostelium* cells incubated in buffer at $t = 0$ and 33 s (*a*) and immobilized in 3% agarose at $t = 0$ and 30 s (*b*). The *white outlines* show the positions of cells at $t = 0$. *Bars* = 10 μm.

on the basis of their brightness and independent of their diffusion times (13, 14). In this study, we have applied FCS to study the diffusion characteristics of PH domain-GFP fusions in the cytoplasm of *Dictyostelium*. PCH analysis has been applied to determine the aggregation state of proteins in the cell.

For our study, we chose three PH domains: PH2, PH10, and the PH domain of CRAC (cytosolic regulator of adenylyl cyclase; referred to as PH-CRAC). PH2 is a domain of an unidentified protein in *Dictyostelium*, the gene of which has not yet been completely described (C4V01S0022.G12).[2] The protein contains two PH domains, one N-terminal and one C-terminal, with a Rho GTPase-activating protein domain in between. PH2 is the C-terminal PH domain. PH10 is the domain of a protein the gene of which has been cloned and is thought to be a novel Akt/protein kinase B homolog (GenBank™/EBI accession number AF093877). PH-CRAC has been studied widely and is known to play a role in the directional response of a cell (5). It transiently translocates to the leading edge of the chemotaxing cell. As an indicator of the intracellular environment, we used free GFP, which is not likely to show nonspecific interactions with intracellular moieties (9), expressed in *Dictyostelium* cytoplasm. The goal of this study was thus to determine the diffusion characteristics of PH2-GFP, PH10-GFP, and PH-CRAC-GFP in *Dictyostelium* cytoplasm to gain a better understanding of the functioning of these domains in the cell and to assess the effect of initiation of chemotaxis on these domains.

EXPERIMENTAL PROCEDURES

Cells—Wild-type *D. discoideum* strain AX3 cells were grown in HG5 medium (14.3 g/liter peptone, 7.15 g/liter yeast extract, 0.54 g/liter Na_2HPO_4, 0.49 g/liter KH_2PO_4, and 10.0 g/liter glucose). For expressing free GFP in the cells, AX3 cells were transfected with the S65T GFP mutant gene cloned into the extrachromosomal expression vector for *Dictyostelium* MB74, which bears a neomycin resistance cassette. The open reading frame of the GFP gene was cloned behind a *Dictyostelium* actin-15 promoter and succeeded by an actin-8 terminator. For expression of the PH domains, the shuffle vector LB3Neo was created. It contains an actin-15 promoter and a Kozak sequence (AAAAATG) succeeded by the S65T GFP gene, which was cloned into the expression vector HK12Neo. LB3Neo also bears a neomycin resistance cassette and has a BglII site, an SpeI site, and a 2H3 terminator behind the GFP gene. For PH10, primers 5′-GCG CCA GAT CTA ATA ATA TGG CAG ATA AAC AAG-3′ (BglII site underlined) and 5′-GCG CGA CTA GTC CAT TTA ATT GTT GAG TTA TAA TCT C-3′ (SpeI site underlined) were used for PCR with genomic *Dictyostelium* DNA as a template. Likewise, PH2 was amplified using primers 5′-GCG GGG GAT CCG AAA TTG TTA AAC AAG GTT A-3′ (BamHI site underlined) and 5′-GCG CCA CTA GTC CTT GTT GTG TTA TAC AAT TTG-3′ (SpeI site underlined). PH2 and PH10 were cloned into the BglII and SpeI sites of LB3Neo using the indicated restriction sites of the primers. The PH-CRAC-GFP construct WF38 was a kind gift of C. A. Parent and P. N. Devreotes. It is also an extrachromosomal *Dictyostelium* expression vector bearing neomycin resistance. The transfected cells were grown in HG5 medium in the presence of 10 μg/ml neomycin (Geneticin, G418 disulfate salt; Sigma). The molecular masses of free GFP and the PH-CRAC-GFP, PH2-GFP, and PH10-GFP fusion proteins are 27, 39, 40, and 39 kDa, respectively.

Sample Preparation—200 or 40 μl of cell suspension was taken from a confluent Petri dish and added to either a LabTek 8-chambered cover glass (Nalge Nunc International Corp.) or a 96-chambered glass bottom microplate (Whatman), respectively. Cells were allowed to settle down for 15–20 min. The medium was then removed, and the cells were washed twice with 17 mM phosphate buffer (pH 6.5). Measurements were performed in cells incubated in buffer. For measurements in polarized cells, the cells were incubated in phosphate buffer for ~5 h. After incubation, the cells had elongated and had started aggregating.

Cell Immobilization—Vegetative cells expressing free GFP were immobilized in a 3% agarose gel (gelling temperature for 2% (w/v) of 36–42 °C; Invitrogen), a solution of which was added to the cells after removing the buffer completely. The agarose solidified in a couple of seconds, reducing the mobility of cells significantly. Fig. 1 compares the movement of cells incubated in buffer with that of cells in agarose. The slow movement of cells in agarose indicates that the cells were alive.

Instrumentation—FCS and PCH measurements were performed with a Zeiss EVOTEC ConfoCor inverted confocal microscope. The details of the setup have been described previously (15, 16). The microscope was equipped with a water immersion objective (C-Apochromat ×40, numerical aperture of 1.2) and a fluorescein filter set (Omega 505 dichroic, 540 DF 50 band-pass filter) to separate the excitation and emission light. The sample was excited at a wavelength of 488 nm from the argon ion laser. The excitation intensity was attenuated with neutral density filters to ~10 microwatts. The pinhole, present for confocal detection, was set at a diameter of 40 μm. The autocorrelation curve was generated with a hardware correlator (ALV-5000E, ALV, Langen, Germany). For PCH analysis, the signal was processed by a dual channel 32-bit PCI photon-counting card (ISS Inc.) (17).

Confocal images of the cells were obtained with a confocal laser scanning microscope (Zeiss ConfoCor 2-LSM 510 combination setup). GFP was excited with the 488-nm argon ion laser controlled by an acousto-optical tunable filter. A dichroic beam splitter (HFT 488) separated the excitation from the emission. The GFP fluorescence was filtered through a band-pass 505–550-nm filter. The objective used was a ×40 oil immersion Plan-Neofluar with a numerical aperture of 1.3. The pinhole was set at 73 μm. Images were analyzed with the Zeiss LSM Image Browser software package.

FCS Measurements—Around 100–150 autocorrelation traces were obtained for each cell strain in vegetative and polarized stages. The measurements were made at two to four randomly chosen spots in the cytoplasm of 10–20 different cells of each cell strain. At each spot in the cell cytoplasm, the measurements were repeated three or five times. Only cells that showed high expression and appeared healthy were chosen for the experiment. In cells expressing free GFP, PH-CRAC-GFP, and PH2-GFP, the expression level was too high for FCS measurements. In these cases, the proteins were photobleached to acceptable fluorescence intensity levels before the measurement by exposing the cells to a high intensity laser beam (~8 milliwatts) for <1 s. Typically,

[2] Available at dictybase.org.

for cells incubated in buffer, measurements of 10 s were performed in vegetative cells and 5 s in polarized cells. Measurements of 20–30 s were made in cells immobilized in agarose. Diffusion of GFP in 17 mM phosphate buffer (pH 8) containing 50% sucrose was also measured under similar experimental conditions as those employed for cellular measurements. Around 100 autocorrelation curves were collected for a measurement time of 10 s.

PCH Measurements—The data were obtained from *Dictyostelium* cells expressing free GFP and PH10-GFP and incubated in 17 mM phosphate buffer (pH 6.5). Single measurements were made in 20 cells of each strain. Raw data were obtained in photon mode. 2×10^6 photons for cells with free GFP and 1×10^6 for cells expressing PH10-GFP were collected at sampling frequencies of 2 and 1 MHz, respectively.

Data Analysis—The autocorrelation traces were analyzed with FCS Data Processor Version 1.3 (Scientific Software Technologies Centre, Department of Systems Analysis, Belarusian State University, Minsk, Belarus). The analysis was performed using the global analysis approach, where five or six autocorrelation traces were fitted simultaneously with their diffusion times (T_{dif}) and triplet lifetimes (T_{trip}) linked. The traces were fitted with a fixed value of the structural parameter (*sp*) that was obtained from calibration with a rhodamine 110 solution and varied between 8 and 12. The structural parameter is defined as the ratio of axial (ω_z) to radial (ω_{xy}) radii of the sample volume element. The average number of molecules (N) and the fractional population of the triplet state (F_{trip}) were allowed to vary. An offset term was added to take into account artifacts in the autocorrelation due to drift in average fluorescence intensity on time scales of >1 s, possibly arising from cellular and intracellular movement (12). The quality of the fit was judged by the reduced χ^2 criterion and by visual inspection of the residuals. Because all measurements were made in the cell cytoplasm, the autocorrelation function ($G(\tau)$) was fit to Equation 1, which describes the three-dimensional Brownian motion of a single species.

$$G(\tau) = 1 + \frac{1}{N}\left(\frac{1}{1+\tau/T_{dif}}\right)\left(\frac{1}{1+(\tau/(T_{dif}sp^2))}\right)^{\frac{1}{2}}\left(1+\frac{F_{trip}e^{-\tau/T_{trip}}}{1-F_{trip}}\right) + \text{offset} \quad \text{(Eq. 1)}$$

The translational diffusion coefficient (D) was calculated from T_{dif} using Equation 2.

$$D = \frac{\omega_{xy}^2}{4T_{dif}} \quad \text{(Eq. 2)}$$

The intracellular viscosity was calculated according to the Stokes-Einstein equation (Equation 3),

$$D = \frac{kT}{6\pi\eta r} \quad \text{(Eq. 3)}$$

where k is the Boltzmann constant, T is the temperature, η is the viscosity of the solution, and r is the hydrodynamic radius of the solute.

The raw data for PCH analysis were acquired and analyzed using Alba FCS Version 2.55 (ISS Inc.). The data were analyzed at a sampling frequency of 50 kHz and fit assuming single species. The PCH function for an open system describes the possibility of observing k photon counts per sampling time, with N as the average number of molecules in the detection volume (13). The molecular brightness (ε), expressed as kilohertz/molecule, is the ratio of the average number of photon counts ($\langle k \rangle$) received per second to N (Equation 4).

$$\varepsilon = \frac{\langle k \rangle}{N} \quad \text{(Eq. 4)}$$

ε is independent of the sampling frequency, and values from different experiments can be directly compared (13).

RESULTS

Localization of PH Domain-GFP Fusions and Free GFP in Cells—Confocal images showing the localization of PH domain-GFP fusions and free GFP in vegetative *Dictyostelium* cells are shown in Fig. 2. PH2-GFP and free GFP were homogeneously distributed in the cell, whereas PH-CRAC-GFP and PH10-GFP transiently localized to parts of the membrane. Fig. 3 shows the translocation of PH10-GFP to a macropinosome in a vegetative cell. In polarized cells, PH10-GFP translocated to the leading edge of the cell (Fig. 4). The distribution of free GFP and PH2-GFP in polarized cells remained similar to that in vegetative cells.

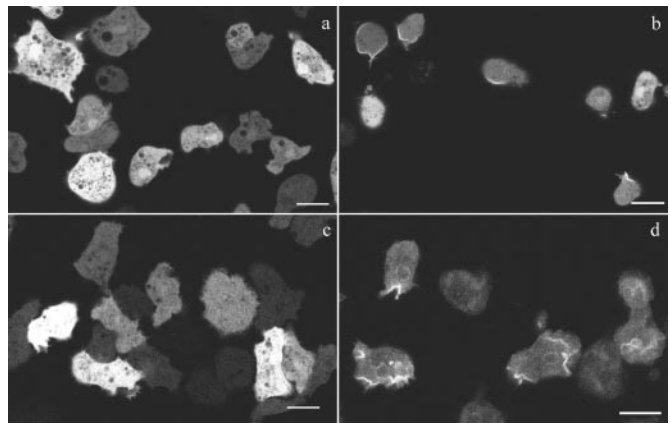

FIG. 2. **Vegetative *Dictyostelium* cells.** Shown are confocal images of cells expressing free GFP (*a*), PH-CRAC-GFP (*b*), PH2-GFP (*c*), and PH10-GFP (*d*). Cells were incubated in buffer. *Bars* = 10 μm.

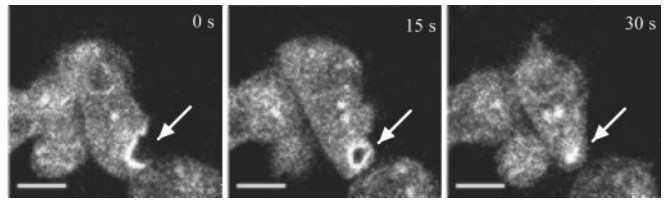

FIG. 3. **Translocation of PH10-GFP to a macropinosome in *Dictyostelium* cells.** The *arrows* point to the macropinosomes. Cells were incubated in buffer. *Bars* = 5 μm.

Diffusion Characteristics in Vegetative Cells—The distributions of diffusion coefficient values for free GFP and PH domain-GFP fusions in vegetative *Dictyostelium* cells incubated in buffer are plotted in Fig. 5 (*b–e*). For comparison with *in vitro* values, the distribution of diffusion coefficient values for GFP in 17 mM phosphate buffer (pH 8) containing 50% sucrose, obtained under similar experimental conditions as used for the cellular measurements, is plotted in Fig. 5*a*. The diffusion coefficient distributions of PH-CRAC-GFP and PH2-GFP overlapped with that of free GFP, whereas that of PH10-GFP showed smaller diffusion coefficient values. The width of the distribution of diffusion coefficient values for GFP and the fusion proteins in cells was larger than for GFP in solution. An estimate of the width can also be obtained from the relative S.D. associated with each average value. The numerical average diffusion coefficients, S.D. values, confidence intervals, and relative S.D. values as determined for each protein and for GFP *in vitro* are listed in Table I. The relative S.D. values for free GFP and PH domain-GFP fusions are between 18 and 20%, whereas that for free GFP *in vitro* is 5%. From the average diffusion coefficient obtained for free GFP in cells and buffer, the average intracellular viscosity in the vegetative cells was calculated to be 3.5 ± 0.7 centipoise (Equation 3).

PH10-GFP Is Not Aggregating—PCH measurements were performed to determine whether the slow diffusion of PH10-GFP could be caused by aggregation of the protein. PCH analysis uses the intensity amplitude distributions to give a quantitative description of the molecular brightness values for the fluorescent species present in the sample. In the autocorrelation curve, this amplitude information can be obtained only from $G(0)$. The molecular brightness of PH10-GFP in vegetative *Dictyostelium* cells was determined and compared with the molecular brightness of free GFP in the cells. The measurements gave an average molecular brightness of 3.7 ± 1.3 kHz/

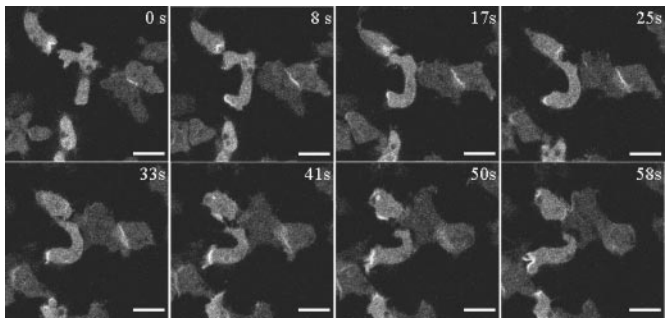

FIG. 4. **Translocation of PH10-GFP to the leading edge of polarized *Dictyostelium* cells.** Cells were incubated in 17 mM phosphate buffer (pH 6.5) for ~5 h. *Bars* = 10 μm.

molecule for PH10-GFP and of 3.1 ± 0.9 kHz/molecule for free GFP. A representative histogram is shown in Fig. 6. The similar molecular brightness for the two proteins indicates that PH10-GFP is not aggregating.

Diffusion Characteristics in Polarized Cells—The effect of polarization on the distributions of diffusion coefficients for PH domain-GFP fusions and free GFP is shown in Fig. 7. PH2-GFP and free GFP showed faster diffusion in polarized cells, as indicated by the shift in the diffusion coefficient distribution of the two proteins to higher values with respect to the distribution in vegetative cells. That the differences in these distributions are significant was confirmed by the unpaired *t* test ($p < 0.005$). The shift was more pronounced for free GFP than for PH2-GFP. However, the diffusion coefficient distributions of PH-CRAC-GFP and PH10-GFP totally overlapped with those obtained in vegetative cells. The unpaired *t* test gave $p > 0.5$. The numerical average diffusion coefficient values are listed in Table I. The relative S.D. associated with each value is between 17 and 22%, similar to the results in vegetative cells. From the average diffusion coefficient obtained for free GFP in the polarized cells, the intracellular viscosity was calculated to be 2.1 ± 0.4 centipoise, ~1.7 times lower than in vegetative cells.

Cellular Movement and Autofluorescence—*Dictyostelium* cells incubated in buffer moved around continuously. The vegetative cells showed random pseudopod formation, and the movement of cells in this stage was slower than the movement of cells in the polarized stage. Measurement times of 10 s for vegetative cells and 5 s for the polarized cells were chosen. This ensured that the cells did not move excessively during the measurement. Even during the chosen time, the fluorescence fluctuations did not remain steady around an average value, probably due to cellular or intracellular movement. A comparison of the intensity traces obtained from GFP diffusion in buffer containing 50% sucrose and GFP diffusion in cells is shown in Fig. 8. The autocorrelation curves obtained from cells could be fit well to the model describing three-dimensional Brownian motion for a single species after an offset term had been added to it (Equation 1). The offset term was needed to account for the slow intensity drifts. Fig. 9 shows a representative autocorrelation curve with the fit and the residuals of the fit.

To estimate the contribution of cellular movement to the widening of the diffusion coefficient distributions obtained from measurements in the cells, autocorrelation traces were also obtained from free GFP-expressing vegetative cells immobilized in agarose. Longer measurement times of 20–30s were possible here. The numerical average diffusion coefficient for free GFP in the immobilized cells is 24 ± 4 $\mu m^2/s$, with the S.D. corresponding to 17% of the average diffusion coefficient value (Table I). The relative S.D. is similar to that obtained for the various cell strains incubated in buffer, indicating that the

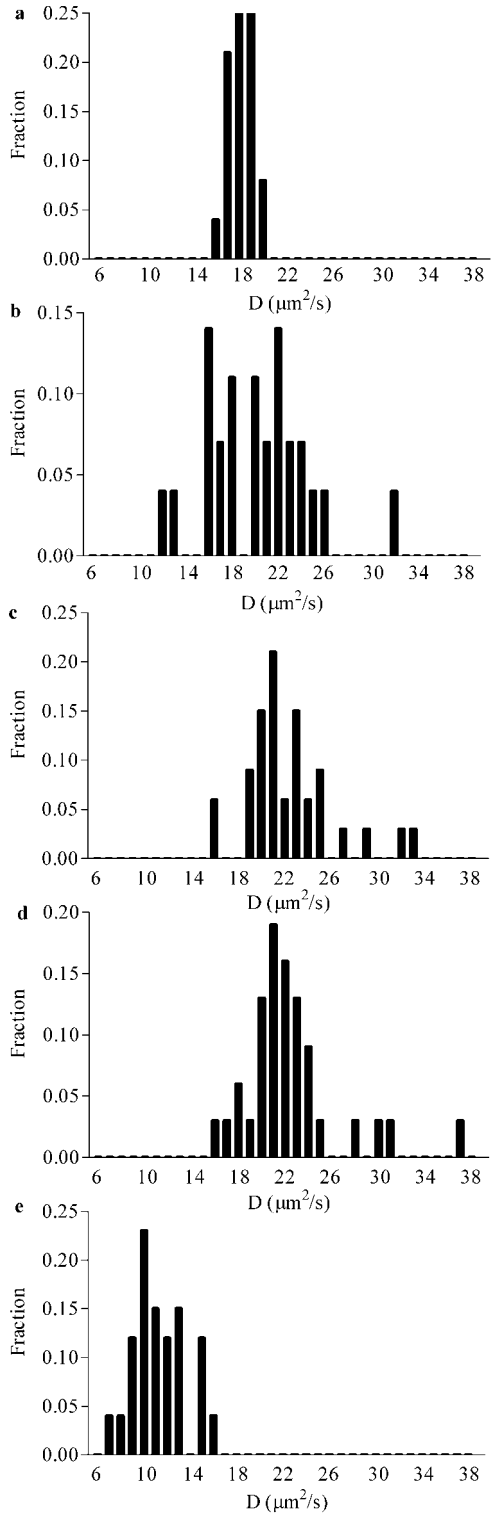

FIG. 5. **Distribution of diffusion coefficients *in vitro* and in vegetative cells.** *a*, GFP in 17 mM phosphate buffer (pH 8) containing 50% sucrose; *b–e*, free GFP, PH-CRAC-GFP, PH2-GFP, and PH10-GFP in vegetative cells, respectively.

movement of the cells does not contribute significantly to the S.D. values associated with the measurements. Also in the case of immobilized cells, slow drifts in fluorescence intensity were seen, probably indicating intracellular movement.

The contribution of cellular autofluorescence was determined from measurements made in wild-type *Dictyostelium* strain AX3 cells. The autofluorescence did not autocorrelate

TABLE I

Diffusion of PH domain-GFP fusions and free GFP in cells and in vitro

Average diffusion coefficients (D), S.D. values, 95% confidence intervals (CI), and relative S.D. (R.S.D.) values were determined for free GFP and PH domain-GFP fusions in the cytoplasm of vegetative and polarized cells and for GFP in 17 mM phosphate buffer (pH 8) containing 50% sucrose

Sample	Vegetative cells			Polarized cells		
	D	CI	R.S.D.	*D*	CI	R.S.D.
	$\mu m^2/s$		%	$\mu m^2/s$		%
Cells incubated in buffer						
Free GFP	20 ± 4	18–22	20	32 ± 6	29–35	19
PH-CRAC-GFP	22 ± 4	21–24	18	23 ± 4	21–25	17
PH2-GFP	22 ± 4	21–24	18	27 ± 6	24–29	22
PH10-GFP	11 ± 2	10–12	18	12 ± 2	11–13	17
Cells immobilized in 3% agarose						
Free GFP	24 ± 4	22–25	17			
In vitro						
GFP	18 ± 1	18–19	5			

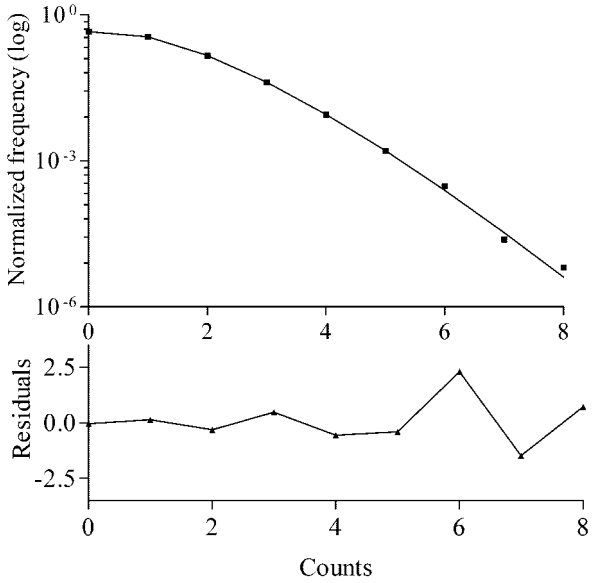

FIG. 6. **PCH of PH10-GFP.** The *upper panel* shows experimental data (■) and the theoretical fit (——); the *lower panel* shows the normalized residuals of the fit. PH10-GFP gave an average brightness value of 3.7 ± 1.3 kHz/molecule.

and hence did not interfere with the measurement of diffusion times. It was thus ignored.

DISCUSSION

The diffusion characteristics of PH2-GFP, PH10-GFP, and PH-CRAC-GFP in the cytoplasm of vegetative and polarized *Dictyostelium* cells have been characterized to obtain a better understanding of the functioning of these domains in the cell and to study the effect of initiation of chemotaxis on these domains. The diffusion of the PH domain-GFP fusions was compared with the diffusion of free GFP in the cells. Free GFP was homogeneously distributed in the *Dictyostelium* cytoplasm (Fig. 2*a*). Of the three PH domains studied, PH2-GFP was homogeneously distributed in the cytoplasm in vegetative cells (Fig. 2*c*) and did not show change in localization upon cell polarization. This indicates that the role of PH2 in the signaling pathway in *Dictyostelium* might be other than membrane recruitment of the protein bearing it. Because it remains cytosolic in polarized cells, it is possible that PH2, like some other PH domains (3, 18), binds to soluble inositol phosphates and perform functions such as negative regulation of signaling pathways by reducing the amount of free inositol phosphates available for other processes. PH10-GFP and PH-CRAC-GFP showed transient translocation to macropinosomes in vegetative cells (Fig. 3) and to the leading edge of the polarized cell

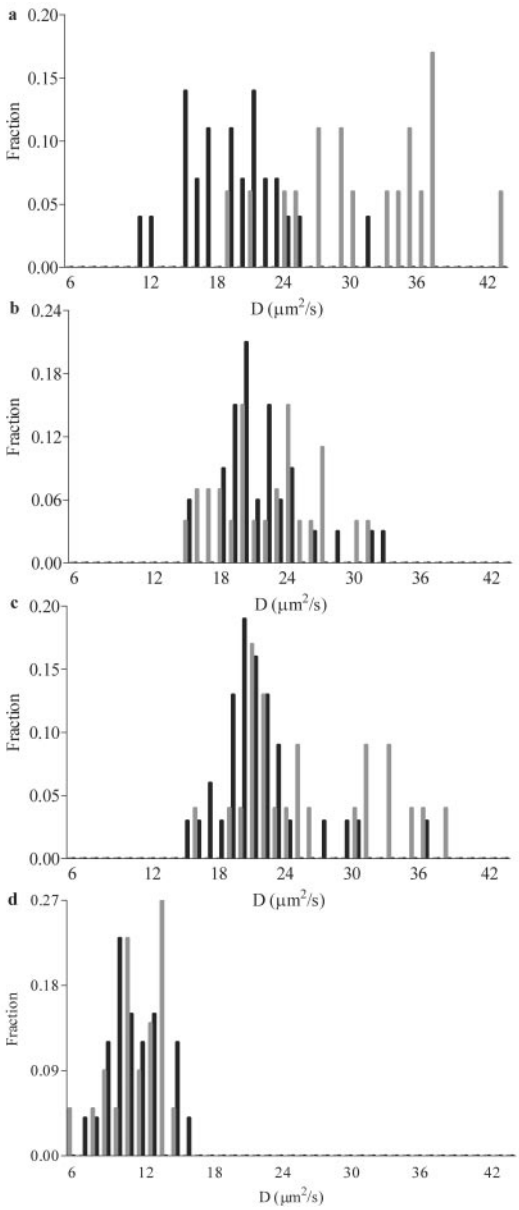

FIG. 7. **Effect of cell polarization on diffusion coefficient distributions of free GFP and PH domain-GFP fusions.** *a–d*, free GFP, PH-CRAC-GFP, PH2-GFP, and PH10-GFP in vegetative (*black bars*) and polarized (*gray bars*) cells, respectively.

(Fig. 4) (19). Thus, PH-CRAC and PH10 are involved in membrane binding in *Dictyostelium*, whereas PH2 is not. However, the diffusion characteristics of PH2-GFP and PH-CRAC-GFP

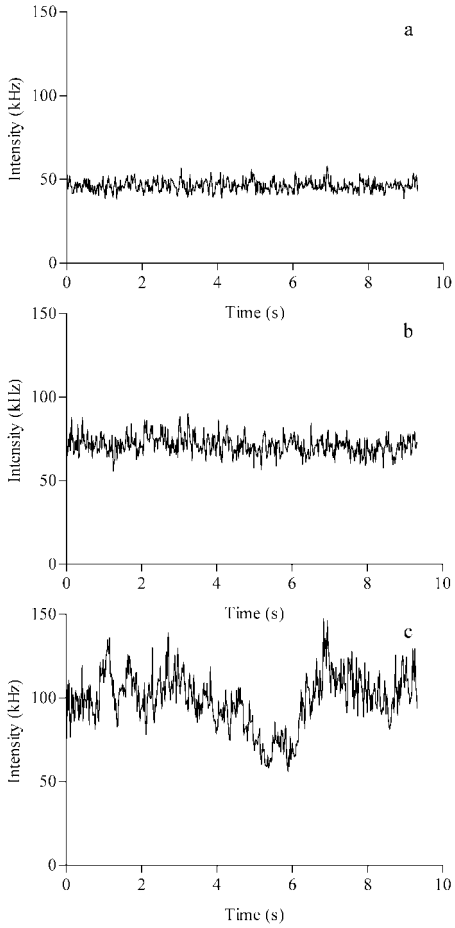

FIG. 8. **Fluorescence intensity traces.** Shown are uniform fluctuations obtained from GFP in phosphate buffer containing 50% sucrose (*a*) and from GFP in the cell cytoplasm (*b*) and non-uniform fluctuations from GFP in the cell cytoplasm (*c*).

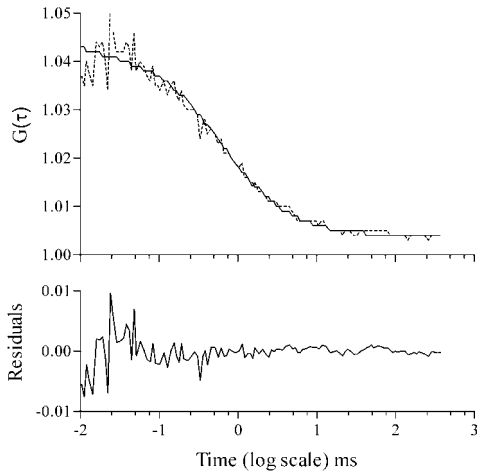

FIG. 9. **Representative autocorrelation curve.** *Upper panel*, autocorrelation curve from a 10-s measurement of PH2-GFP diffusion in the cytoplasm of vegetative cells. – – –, experimental curve; ——, theoretical fit. *Lower panel*, residuals of the fit.

in vegetative cells were very similar. Their diffusion coefficient distributions also overlapped with that of free GFP. This is expected, as the molecular mass of GFP differs from that of the PH domain-GFP fusions only by a factor of 1.5. With FCS, it is not possible to distinguish between two species in an identical environment without *a priori* knowledge until the molecular masses differ by a factor of 4 at least (20). Free GFP, which lacks nonspecific interactions with cellular moieties (9), is a good indicator of the intracellular environment. The similarity in the diffusion characteristics of PH2-GFP and PH-CRAC-GFP with those of free GFP indicates that the two PH domains are not interacting with any bulky intracellular moiety in the cytosol. It is surprising that the diffusion of PH10-GFP was slower than that of the other PH domains and free GFP. With PCH analysis, it has been shown that this slow diffusion is not due to aggregation of the protein. A possible reason for the slow diffusion of PH10-GFP could be that the domain is interacting with a bulky intracellular moiety, ~8 times its molecular mass, because the diffusion is twice as slow as that of the other PH domains or that it is enclosed in high viscosity microregions formed by the cytoskeleton in the cytoplasm. Luby-Phelps *et al.* (21) have demonstrated the presence of structural barriers in the form of filamentous meshwork of varying pore sizes in the cytoplasm.

The diffusion coefficients obtained from measurements at different positions in cells show wide distributions compared with GFP *in vitro* (Figs. 5 and 7). The wide distributions illustrate the heterogeneity and dynamics of the intracellular environment. From the width of the distributions and relative S.D. values for the PH domain-GFP fusions and free GFP in the cells (Table I), it is clear that the intracellular heterogeneities affected all the species to a similar extent. The effect was also similar in vegetative and polarized cells. However, the changes in the intracellular environment upon polarization of the cell affected free GFP and the three PH domain-GFP fusions differently. The diffusion of free GFP in the cell cytoplasm was faster in polarized cells than in vegetative cells, as indicated by the shift in the distribution of the diffusion coefficient values to higher values (Fig. 7). The diffusion coefficients obtained for free GFP in buffer and cells indicate that the intracellular viscosity in polarized cells was ~1.7 times lower than in vegetative cells. A 1.4-fold decrease in the cytoplasmic viscosity in polarized *Dictyostelium* cells was observed in a previous study using FRAP (6). Faster diffusion was also seen for PH2-GFP in polarized cells, although, in this case, the shift in the distribution of diffusion coefficient values was less pronounced. Surprisingly, PH10-GFP and PH-CRAC-GFP showed no change in their diffusion characteristics upon polarization of the cells. Thus, the lowering of viscosity had no detectable effect on PH10-GFP and PH-CRAC-GFP diffusion. This can be the case if the effect of change in viscosity on PH10 and PH-CRAC diffusion is cancelled by another event taking place in the polarized cells. At this stage, it is not clear what that event might be.

The factors that can interfere with FCS measurements are cellular autofluorescence and fluorophore depletion in the cell because of photodestruction at the focus (22). An additional factor in *Dictyostelium* is the movement of the cells. Below, it is shown that these three factors did not interfere with our measurements. The autofluorescence from the cells did not correlate and so did not contribute to the autocorrelation function derived from the diffusion of GFP and GFP fusion proteins. Thus, it did not interfere with the measurement of diffusion times and was ignored. The second factor, *i.e.* the possibility of photodestruction in the excitation volume during the measurement, was minimized by using short measurement times (5–10 s) at low excitation intensities (<10 microwatts). The expression levels of cells with free GFP, PH-CRAC-GFP, and PH2-GFP were too high for FCS, and so the fluorophore was bleached before the measurement. However, no fluorescence recovery or photobleaching was observed during the measurement. This indicates that the average number of molecules in the detection volume remained constant. Consequently, the

diffusion times were not affected by the bleaching procedure. The third factor that has to be taken into account is the high mobility of *Dictyostelium* cells. Cells incubated in buffer constantly formed pseudopods and moved around. This made it difficult to make repeated measurements in these cells. The measurement times chosen for the experiments (5–10 s) not only minimized the possibility of photodepletion, but also ensured that the movement of the cells during the measurement was limited. Longer measurement times of up to 30 s were possible in cells immobilized in agarose. For most of the measurements, it was observed that the average fluorescence intensity did not remain steady around an average value, but showed a slow drift (Fig. 8). This also held true for cells immobilized in agarose. Similar drifts in average fluorescence intensity obtained from the cytoplasm have been observed in other cells (10). The slow drifts in intensity on the time scale of seconds were attributed to cellular and intracellular movements. The drifts were accounted for by adding an offset value to the autocorrelation curve (Equation 1).

In conclusion, we have characterized the diffusion of three PH domains in *Dictyostelium* cells. Of the three domains, PH2 was homogeneously distributed in vegetative and polarized cells, whereas PH10 and PH-CRAC showed transient translocation to the leading edge of the polarized cell. The diffusion characteristics of PH2 and PH-CRAC in vegetative cells were very similar, but PH10 exhibited slower diffusion. All three PH domains were similarly affected by the intracellular heterogeneities. However, in polarized cells, where the viscosity was 1.7 times lower than in vegetative cells, only PH2 showed increased mobility. PH10 and PH-CRAC did not show any change.

REFERENCES

1. Firtel, R. A., and Chung, C. Y. (2000) *BioEssays* **22,** 603–615
2. Bottomley, M. J., Salim, K., and Panayotou, G. (1998) *Biochim. Biophys. Acta* **1436,** 165–183
3. Hirata, M., Kanematsu, T., Takeuchi, H., and Yagisawa, H. (1998) *Jpn. J. Pharmacol.* **76,** 255–263
4. Lemmon, M. A., and Ferguson, K. M. (2000) *Biochem. J.* **350,** 1–18
5. Parent, C. A., and Devreotes, P. N. (1999) *Science* **284,** 765–770P. N.
6. Potma, E. O., de Boeij, W. P., Bosgraaf, L., Roelofs, J., van Haastert, P. J., and Wiersma, D. A. (2001) *Biophys. J.* **81,** 2010–2019
7. Hess, S. T., Huang, S., Heikal, A. A., and Webb, W. W. (2002) *Biochemistry* **41,** 697–705
8. Schwille, P., Haupts, U., Maiti, S., and Webb, W. W. (1999) *Biophys. J.* **77,** 2251–2265
9. Dittrich, P., Malvezzi Campeggi, F., Jahnz, M., and Schwille, P. (2001) *Biol. Chem.* **382,** 491–494
10. Chen, Y., Muller, J. D., Ruan, Q., and Gratton, E. (2002) *Biophys. J.* **82,** 133–144
11. Wachsmuth, M., Waldeck, W., and Langowski, J. (2000) *J. Mol. Biol.* **298,** 677–689
12. Brock, R., Vamosi, G., Vereb, G., and Jovin, T. M. (1999) *Proc. Natl. Acad. Sci. U. S. A.* **96,** 10123–10128
13. Chen, Y., Muller, J. D., So, P. T., and Gratton, E. (1999) *Biophys. J.* **77,** 553–567
14. Müller, J. D., Chen, Y., and Gratton, E. (2000) *Biophys. J.* **78,** 474–486
15. Hink, M. A., van Hoek, A., and Visser, A. J. W. G. (1999) *Langmuir* **15,** 992–997
16. Hink, M. A., Borst, J. W., and Visser, A. J. W. G. (2003) *Methods Enzymol.* **361,** 93–112
17. Eid, J. S., Muller, J. D., and Gratton, E. (2000) *Rev. Sci. Instrum.* **71,** 361–368
18. Varnai, P., Lin, X., Lee, S. B., Tuymetova, G., Bondeva, T., Spat, A., Rhee, S. G., Hajnoczky, G., and Balla, T. (2002) *J. Biol. Chem.* **277,** 27412–27422
19. Parent, C. A., Blacklock, B. J., Froehlich, W. M., Murphy, D. B., and Devreotes, P. N. (1998) *Cell* **95,** 81–91
20. Meseth, U., Wohland, T., Rigler, R., and Vogel, H. (1999) *Biophys. J.* **76,** 1619–1631
21. Luby-Phelps, K., Taylor, D. L., and Lanni, F. (1986) *J. Cell Biol.* **102,** 2015–2022
22. Brock, R., and Jovin, T. M. (2001) in *Fluorescence Correlation Spectroscopy: Theory and Applications* (Rigler, R., and Elson, E. S., eds) pp. 132–161, Springer-Verlag, Berlin